Hindawi Publishing Corporation
Advances in High Energy Physics
Volume 2014, Article ID 639759, 13 pages
http://dx.doi.org/10.1155/2014/639759

Hindawi

Research Article

Schwarzschild-de Sitter and Anti-de Sitter Thin-Shell Wormholes and Their Stability

M. Sharif and Saadia Mumtaz

Department of Mathematics, University of the Punjab, Quaid-e-Azam Campus, Lahore 54590, Pakistan

Correspondence should be addressed to M. Sharif; msharif.math@pu.edu.pk

Received 19 June 2014; Revised 22 August 2014; Accepted 22 August 2014; Published 9 September 2014

Academic Editor: Rong-Gen Cai

This paper is devoted to construct Schwarzschild-de Sitter and anti-de Sitter thin-shell wormholes by employing Visser's cut and paste technique. The Darmois-Israel formalism is adopted to formulate the surface stresses of the shell. We analyze null and weak energy conditions as well as attractive and repulsive characteristics of thin-shell wormholes. We also explore stable and unstable solutions against linear perturbations by taking two different Chaplygin gas models for exotic matter. It is concluded that the stress-energy tensor components violate the null and weak energy conditions indicating the existence of exotic matter at the wormhole throat. Finally, we find unstable and stable configurations for the constructed thin-shell wormholes.

1. Introduction

A wormhole is a hypothetical region of spacetime which acts as a shortcut connecting different regions of the universe through a handle or tunnel. The word "wormhole," also known as Einstein-Rosen bridge, was first investigated by Einstein and Rosen [1]. The occurrence of event horizon prevents the traversable motion across distant regions of the universe through this wormhole. Morris and Thorne [2] suggested traversable wormhole solution which has no event horizon and enables the observers to traverse across both universes.

Traversable wormholes are made up of two asymptotically flat regions which are associated by a throat and satisfy the flare-out condition to conserve the wormhole geometry. The violation of null (NEC) and weak energy conditions (WEC) is the fundamental property for traversable wormholes indicating the occurrence of exotic matter which must be fulfilled at the wormhole throat. The physical evidence of wormholes is a debatable issue due to exotic matter at the throat. Null energy condition is the weakest condition whose violation leads to the violation of WEC as well as strong energy condition (SEC). We characterize exotic matter by the stress-energy tensor components formulated by applying the Darmois-Israel formalism [3, 4]. It was proposed [5] that the violation of NEC can be minimized by applying the cut and paste procedure to construct a spherically symmetric thin-shell wormhole (TSW). The exotic matter was restricted at the edges and corners of the wormhole throat so that an observer could easily travel without encountering it.

It has always been fascinating to explore the stability issue of different solutions of the field equations. Different stability phases of the celestial objects give rise to various evolutionary mechanisms in the universe [6, 7]. Traversable wormholes are of remarkable significance if they are stable under linear perturbations preserving the symmetry. The stable/unstable wormhole models can be analyzed either by taking perturbations around a static solution or by using equation of state (EoS) for exotic matter at the wormhole throat. In this context, Poisson and Visser [8] investigated stable TSWs against linear perturbations formed by joining two different manifolds of the Schwarzschild geometry. Lobo and Crawford [9] extended this analysis for spherically symmetric TSWs with cosmological constant (Λ) and found that positive Λ increases the stability regions but this region decreases for negative Λ.

Thibeault et al. [10] studied stable 5D wormhole configurations with Gauss-Bonnet term in Einstein-Maxwell theory. Amirabi et al. [11] analyzed the effects of Gauss-Bonnet term on wormhole stability in higher dimensions. Sharif and

Yousaf [12] found some stable wormhole solutions due to $R + \epsilon R^2$ gravity. Eiroa and Simeone [13] explored only unstable cylindrical TSWs from local cosmic strings. Richarte [14] studied these solutions by invoking Chaplygin as well as anti-Chaplygin gases with $\Lambda > 0$. Recently, we have constructed charged black string wormhole configurations and examined stable TSWs [15].

In order to explore some realistic sources for exotic matter at the wormhole throat, a lot of work has been done by taking various candidates like phantom energy [16, 17], tachyon matter [18], and Chaplygin gas [19, 20]. Eiroa [21] constructed spherical TSWs in the context of generalized Chaplygin gas (GCG). Kuhfittig [22] discussed the stability of spherical TSWs in the presence of Λ and charge by considering phantomlike EoS at the throat. Bandyopadhyay et al. [23] investigated the stability of TSWs supported by modified Chaplygin gas (MCG). Banerjee [24] explored stability formalism for (2+1)-dimensional spherical TSWs by taking phantom energy and Chaplygin gas as an exotic matter. Sharif and Azam have investigated both stable and unstable spherical TSWs by using modified generalized Chaplygin gas (MGCG) [25] and generalized cosmic Chaplygin gas (GCCG) [26].

This paper is devoted to analyze the stability of spherical TSWs in the presence of Λ by taking two different EoSs for exotic matter. The paper is arranged in the following way. In Section 2, we implement Visser's cut and paste approach to construct Schwarzschild-de Sitter and anti-de Sitter TSWs and discuss different physical aspects of these constructed TSWs. A general linearized formalism for stability is developed in Section 3. This analysis is applied to the constructed TSWs in Section 4. The last section deals with the conclusions of our results.

2. General Formalism

In this section, we provide a basic formalism to construct spherical TSWs. The static spherically symmetric spacetime with nonvanishing Λ is given by

$$ds^2 = -G(r)\,dt^2 + G^{-1}(r)\,dr^2 + H(r)\left(d\theta^2 + \sin^2\theta d\phi^2\right), \tag{1}$$

where $G(r) = 1 - (2M/r) - (\Lambda r^2/3)$ and $H(r) = r^2$. For $\Lambda > 0$, this gives Schwarzschild-de Sitter, $\Lambda < 0$ leads to Schwarzschild-anti-de Sitter, and $\Lambda = 0$ yields Schwarzschild metric. Since $G(r) < 0$ for $\Lambda M^2 > 1/9$, so we must have $0 < \Lambda M^2 \leq 1/9$, which leads to two roots, the event horizon r_h and the cosmological horizon r_c for the Schwarzschild-de Sitter geometry as follows:

$$r_h = \frac{2}{\sqrt{\Lambda}}\cos\left(\frac{\alpha}{3}\right),$$
$$r_c = \frac{2}{\sqrt{\Lambda}}\cos\left(\frac{\alpha}{3} + \frac{4\pi}{3}\right), \tag{2}$$

where $\cos\alpha = -3M\sqrt{\Lambda}$ with $\pi < \alpha < 3\pi/2$ and the domain $2M < r_h < 3M$ and $r_c > 3M$.

The wormhole construction is not possible for $\Lambda M^2 = 1/9$, because both horizons merge at $r_h = r_c = 3M$. This implies that the wormhole throat radius a_0 must have the range $r_h < a_0 < r_c$ and $0 < \Lambda M^2 < 1/9$ for the static solution. The event horizon for the Schwarzschild-anti-de Sitter geometry is given by

$$\widetilde{r}_h = \left(\frac{3M}{|\Lambda|}\right)^{1/3} \times \left[\sqrt[3]{1 + \sqrt{1 + \frac{1}{9|\Lambda|M^2}}} + \sqrt[3]{1 - \sqrt{1 + \frac{1}{9|\Lambda|M^2}}}\right]. \tag{3}$$

Notice that, for the existence of static wormhole configuration, we must have $\widetilde{r}_h < a_0$ and $0 < \widetilde{r}_h < 2M$.

The cut and paste procedure is a successful way for mathematical construction of TSWs. In this context, the interior region of the given spacetime is cut with $r < a$, yielding two 4D copies $\mathcal{M}^{\pm}$ with $r \geq a$. A new manifold $\mathcal{M} = \mathcal{M}^{+} \cup \mathcal{M}^{-}$ is obtained by joining them at the hypersurface:

$$\Sigma^{\pm} = \Sigma = \{r = a\}. \tag{4}$$

The geometric condition required for the wormhole construction is the fulfillment of flare-out condition by the throat radius; that is, the embedding function $H(r)$ in (1) satisfies the relation $H'(a) = 2a > 0$. The proper radial distance can be defined on the constructed wormhole as $s = \pm\int_a^r \sqrt{(1/G(r))}dr$, which depicts the throat position for $s = 0$. If this construction fulfills the radial flare-out condition, then the new manifold is called geodesically complete and describes a TSW obtained by connecting two regions with radius a, which corresponds to the minimal area hypersurface. We define the coordinates $\xi^i = (\tau, \theta, \phi)$ at Σ, τ the proper time on the shell. The induced 3D metric at Σ is defined as

$$ds^2 = -d\tau^2 + a^2(\tau)\left(d\theta^2 + \sin^2\theta d\phi^2\right). \tag{5}$$

We employ the standard Darmois-Israel formalism [3] to discuss the dynamics of TSWs. The surface stresses at Σ are evaluated by the Einstein equations at Σ, that is, by the Lanczos equations:

$$S_{ij} = \frac{1}{8\pi}\left\{g_{ij}K - \left[K_{ij}\right]\right\}, \tag{6}$$

where $[K_{ij}] = K^{+}_{ij} - K^{-}_{ij}$ and $K = \mathrm{tr}[K_{ij}] = [K^i_i]$. The surface stress-energy tensor $S_{ij} = \mathrm{diag}(\sigma, p_\phi, p_z)$ provides the surface energy density σ and surface tensions $p = p_\phi = p_z$. The extrinsic curvatures $K^{\pm}_{ij}$ joining the two sides of the shell are defined as

$$K^{\pm}_{ij} = -n^{\pm}_{\kappa}\left(\frac{\partial^2 x^{\kappa}_{\pm}}{\partial\xi^i\partial\xi^j} + \Gamma^{\kappa}_{\mu\nu}\frac{\partial x^{\mu}_{\pm}}{\partial\xi^i}\frac{\partial x^{\nu}_{\pm}}{\partial\xi^i}\right), \quad (i, j = 0, 2, 3). \tag{7}$$

The unit four-vector normals $n_\kappa^\pm$ to $\mathscr{M}^\pm$ are defined by

$$n_\kappa^\pm = \pm\left|g^{\mu\nu}\frac{\partial\eta}{\partial x^\mu}\frac{\partial\eta}{\partial x^\nu}\right|^{-1/2}\frac{\partial\eta}{\partial x^\kappa} = \left(-\dot{a}, \frac{\sqrt{G(r)+\dot{a}^2}}{G(r)}, 0, 0\right), \tag{8}$$

satisfying the relation $n^\kappa n_\kappa = 1$. Using (1) and (7), the components of extrinsic curvature are

$$K_{\tau\tau}^\pm = \mp\frac{G'(a)+2\ddot{a}}{2\sqrt{G(a)+\dot{a}^2}}, \qquad K_{\phi\phi}^\pm = \pm a\sqrt{G(a)+\dot{a}^2}, \tag{9}$$
$$K_{zz}^\pm = \alpha^2 K_{\phi\phi}^\pm,$$

where dot and prime correspond to $d/d\tau$ and d/dr, respectively. Using (6) and (9), the surface stresses to Σ yield

$$\sigma = -\frac{1}{2\pi a}\sqrt{G(a)+\dot{a}^2}, \tag{10}$$

$$p = p_\phi = p_z = \frac{1}{8\pi}\frac{2\dot{a}^2+2a\ddot{a}+2G(a)+aG'(a)}{a\sqrt{G(a)+\dot{a}^2}}. \tag{11}$$

We require the following energy conditions, that is, WEC: $\sigma \geq 0$, $\sigma + p \geq 0$, NEC: $\sigma + p \geq 0$, and SEC: $\sigma + p \geq 0$, $\sigma + 3p \geq 0$. We see from (10) and (11) that $\sigma < 0$ and $\sigma + p < 0$, which shows the violation of NEC and WEC for different values of M and a, leading to the occurrence of exotic matter at the shell $r = a$. The violation of the energy conditions corresponding to both spherical TSWs is shown in Figure 1.

Now, we investigate the attractive and repulsive nature of the constructed TSWs. For this purpose, we have to calculate the observer's four-acceleration:

$$a^\mu = u^\mu_{;\nu}u^\nu, \tag{12}$$

where $u^\mu = dx^\mu/d\tau = (1/\sqrt{G(r)}, 0, 0, 0)$ is the observer's four-velocity. The nonzero component of four-acceleration for (1) is given by

$$a^r = \Gamma^r_{tt}\left(\frac{dt}{d\tau}\right)^2 = \frac{M}{r^2} - \frac{\Lambda r}{3}, \tag{13}$$

for which the geodesic equation of motion has the form

$$\frac{d^2r}{d\tau^2} = -\Gamma^r_{tt}\left(\frac{dt}{d\tau}\right)^2 = -a^r. \tag{14}$$

It is worth mentioning here that a wormhole has attractive nature if $a^r > 0$; that is, an observer must move with an outward-directed radial acceleration in order to avoid being dragged by the wormhole. The wormhole is repulsive for $a^r < 0$; that is, an observer must have the radial acceleration directed towards inside in order to keep away from being pushed by the wormhole [22, 24]. The attractive and repulsive characteristics of the spherical TSWs are shown in Figure 2.

For large values of Λ, M, and a_0, a surface tension is needed to support or hold the wormhole from expanding, so that a traveler can easily traverse through it. For low values of Λ, M, and a_0, the surface pressure p_0 prevents the wormhole from expanding. The corresponding results are shown in Figure 3.

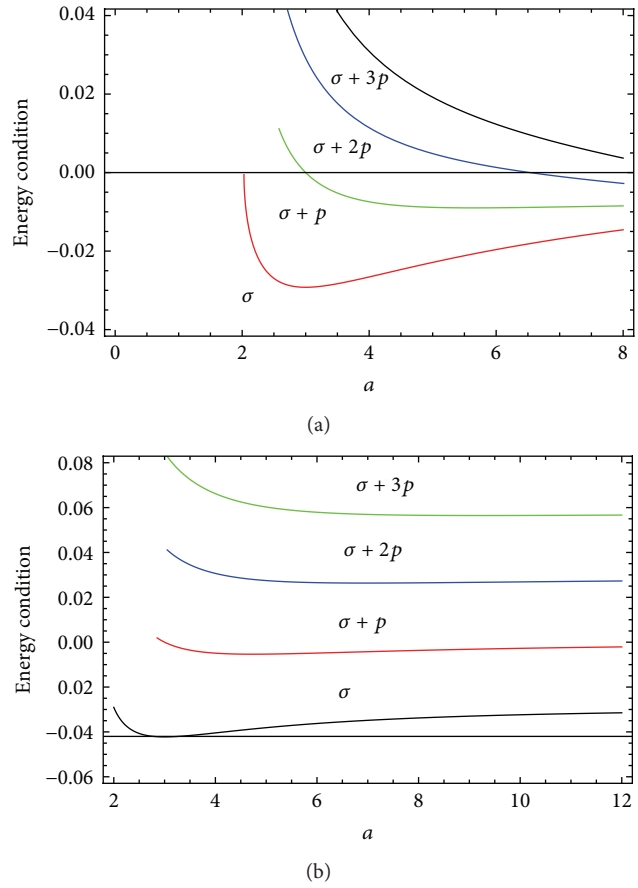

Figure 1: Plots of energy conditions for TSWs corresponding to $M = 1$, $\Lambda = 0.01$ (a) and $M = 1$, $\Lambda = -0.1$ (b).

3. Standard Approach for Stability Analysis

This section deals with the wormhole stability through linear perturbations. The corresponding surface stresses, that is, σ and p, for the static wormhole solutions ($\dot{a} = \ddot{a} = 0$) using (10) and (11) turn out to be

$$\sigma_0 = -\frac{\sqrt{G(a_0)}}{2\pi a_0}, \qquad p_0 = \frac{1}{8\pi}\frac{2G(a_0)+a_0G'(a_0)}{a_0\sqrt{G(a_0)}}. \tag{15}$$

The dynamics of throat is described by thin-shell equation of motion which can be obtained by rearranging (10) as $\dot{a}^2 + V(a) = 0$, where $V(a)$ is the potential function given by

$$V(a) = G(a) - [2\pi a\sigma(a)]^2. \tag{16}$$

We observe that σ and p satisfy the conservation equation:

$$\frac{d}{d\tau}(\sigma\Delta) + p\frac{d\Delta}{d\tau} = 0, \tag{17}$$

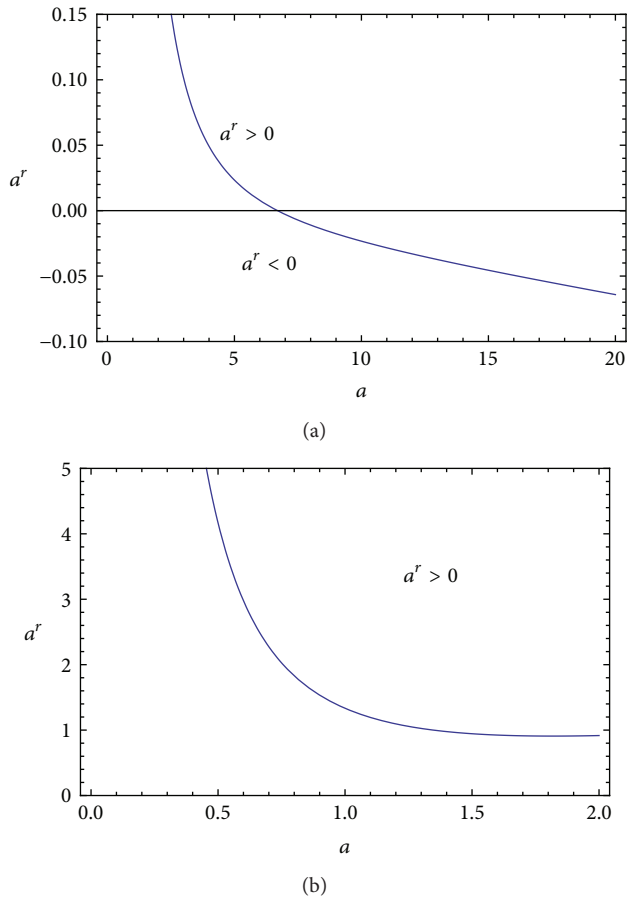

Figure 2: Plots for attractive and repulsive nature of Schwarzschild-de Sitter corresponding to $M = 1$ and $\Lambda = 0.01$ (a) and Schwarzschild-anti-de Sitter with $M = 1$ and $\Lambda = -1$ (b). The wormholes are attractive for $a^r > 0$ and repulsive for $a^r < 0$.

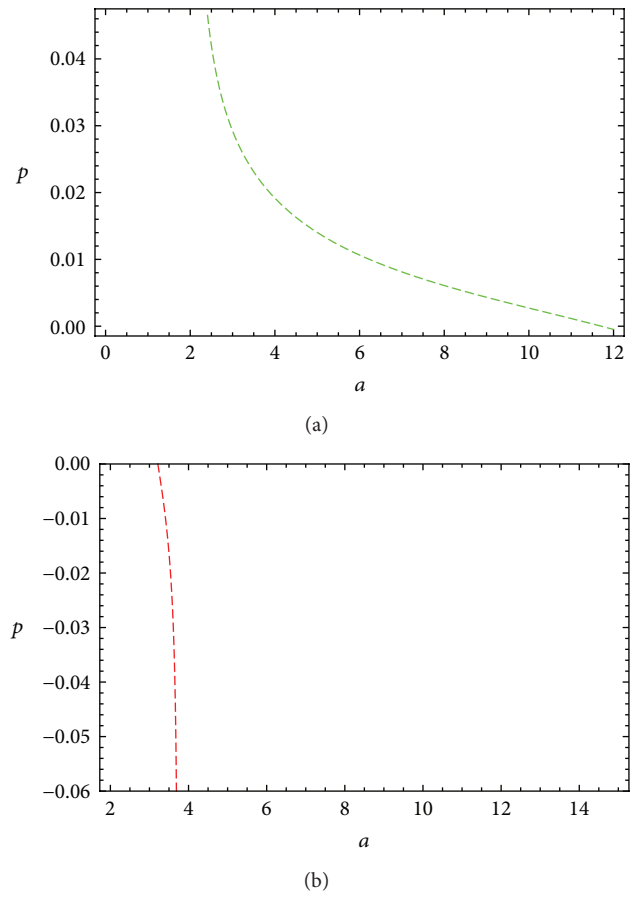

Figure 3: Plots of surface pressure for TSWs corresponding to $M = 0.2$, $\Lambda = -0.1$ (a) and surface tension for $M = 1$, $\Lambda = 0.1$ (b).

where $\Delta = 4\pi a^2$ is the wormhole throat area. This equation can be written as

$$a\sigma' = -2(\sigma + p), \tag{18}$$

where we have used $\sigma' = \dot{\sigma}/\dot{a}$. To investigate the wormhole stability, we expand $V(a)$ by Taylor's series up to second order around $a = a_0$, yielding

$$V(a) = V(a_0) + V'(a_0)(a - a_0) + \frac{1}{2}V''(a_0)(a - a_0)^2 + O\left[(a - a_0)^3\right]. \tag{19}$$

Differentiating (16) and using (18), we have

$$V'(a) = G'(a) + 8\pi^2 a\sigma(a)\left[\sigma(a) + 2p(a)\right]. \tag{20}$$

It is remarked that stability of wormhole static solution depends upon $V'(a_0) = 0 = V(a_0)$ and $V''(a_0) \gtrless 0$.

4. Schwarzschild-de Sitter and Anti-de Sitter Wormholes

Here we construct Schwarzschild-de Sitter as well as anti-de Sitter TSWs. From (15), the surface stresses for static configuration become

$$\sigma_0 = -\frac{\sqrt{3a_0 - 6M - \Lambda a_0^3}}{2\pi a_0\sqrt{3a_0}}, \qquad p_0 = \frac{3a_0 - 3M - 2\Lambda a_0^3}{4\pi a_0\sqrt{3a_0\left(3a_0 - 6M - \Lambda a_0^3\right)}}. \tag{21}$$

The matter violating the null and weak energy conditions is known as exotic matter. In order to explore some realistic sources for exotic matter at the WH throat, a lot of work has been done by taking various candidates of dark energy like family of Chaplygin gas, phantom energy, and quintessence. To support the exotic matter at the wormhole throat, we model wormholes by taking GCCG and modified cosmic Chaplygin gas (MCCG) EoSs in the following subsections.

4.1. Generalized Cosmic Chaplygin Gas. We model the exotic matter with GCCG [27] at the shell to investigate the wormhole dynamics. The EoS for GCCG is defined as

$$p = -\frac{1}{\sigma^{\gamma}}\left[E + \left(\sigma^{1+\gamma} - E\right)^{-w}\right], \tag{22}$$

where $E = B/(1+w) - 1$, $B \in (-\infty, \infty)$, and $-C < w < 0$. Here C is taken as a positive constant other than unity. This EoS corresponds to GCG in the limit $w \to 0$ and the usual Chaplygin gas is recovered for $w = 0, \gamma = 1$. Using (15) in (22), we formulate the following equation for static configuration:

$$\begin{aligned}&\left[a_0^2 G'(a_0) + 2a_0 G(a_0)\right][2a_0]^{\gamma} \\ &\quad - 2\left(4\pi a_0^2\right)^{1+\gamma}[G(a_0)]^{(1-\gamma)/2} \\ &\quad \times \left[E + \left\{(2\pi a_0)^{-(1+\gamma)}(G(a_0))^{(1+\gamma)/2} - E\right\}^{-w}\right] = 0.\end{aligned} \tag{23}$$

By taking the first derivative of (22), we have

$$p'(a) = \sigma'(a)\left[w(1+\gamma)\left\{\sigma^{1+\gamma} - E\right\}^{-(1+w)} - \frac{\gamma p(a)}{\sigma(a)}\right], \tag{24}$$

which leads to

$$\begin{aligned}&\sigma'(a) + 2p'(a) \\ &\quad = \sigma'(a)\left[1 + 2w(1+\gamma)\left\{\sigma^{1+\gamma} - E\right\}^{-(1+w)} - \frac{2\gamma p(a)}{\sigma(a)}\right].\end{aligned} \tag{25}$$

By differentiating (20) and using (25), $V''(a)$ can be written as

$$\begin{aligned}&V''(a) \\ &= G''(a) - 8\pi^2 \\ &\quad \times \left\{[\sigma(a) + 2p(a)]^2 + 2\sigma(a)[\sigma(a) + p(a)]\right. \\ &\qquad \left.\times \left[1 - \frac{2\gamma p}{\sigma} + 2w(1+\gamma)\left(\sigma(a)^{1+\gamma} - E\right)^{-1-w}\right]\right\}.\end{aligned} \tag{26}$$

Inserting the values of $\sigma(a_0)$ and $p(a_0)$ from (15), we see that both $V(a)$ and $V'(a)$ become zero at $a = a_0$, while (26) takes the form

$$\begin{aligned}V''(a_0) &= G''(a_0) + \frac{(\gamma-1)\left[G'(a_0)\right]^2}{2G(a_0)} \\ &\quad + \frac{G'(a_0)}{a_0}\left[1 + 2w(1+\gamma)\right. \\ &\qquad \left.\times \left\{\left(\frac{\sqrt{G(a_0)}}{2\pi a_0}\right)^{1+\gamma} - E\right\}^{-(1+w)}\right] \\ &\quad - \frac{2G(a_0)}{a_0^2}(1+\gamma) \\ &\quad \times \left[1 + 2w\left\{\left(\frac{\sqrt{G(a_0)}}{2\pi a_0}\right)^{1+\gamma} - E\right\}^{-(1+w)}\right].\end{aligned} \tag{27}$$

We are interested to study the stability of Schwarzschild-de Sitter and anti-de Sitter TSWs. In this context, the corresponding dynamical equation for static solution by substituting (21) in (22) takes the form

$$\begin{aligned}&3a_0 - 3M - 2\Lambda a_0^3 - 2\left(2\pi a_0\sqrt{3a_0}\right)^{1+\gamma} \\ &\quad \times \left[3a_0 - 6M - \Lambda a_0^3\right]^{(1-\gamma)/2} \\ &\quad \times \left[E + \left\{\left(2\pi a_0\sqrt{3a_0}\right)^{-(1+\gamma)}\right.\right. \\ &\qquad \left.\left.\times \left(3a_0^4 - 6M - \Lambda a_0^3\right)^{(1+\gamma)/2} - E\right\}^{-w}\right] = 0,\end{aligned} \tag{28}$$

where its solutions represent static spherical TSWs. Equation (27) yields

$$\begin{aligned}&V''(a_0) \\ &= \frac{2}{3a_0^3\left(3a_0 - 6M - \Lambda a_0^4\right)} \\ &\quad \times \left[9M\Lambda a_0^3(2 - a_0) + \Lambda a_0^4(a_0 - 1)\right. \\ &\qquad \times \left[6 - \Lambda a_0^2(a_0 - 1)\right] + 2M(a_0 - M) - 9a_0^2 \\ &\qquad + \gamma\left[\Lambda^2 a_0^6\left(1 - a_0^2\right) - 6M\Lambda a_0^3(1 + 2a_0) + 9M(4a_0 - 3M)\right. \\ &\qquad\quad \left.\left.-9a_0^2\right] + 2(1+\gamma)\right. \\ &\qquad \times \left\{3M\Lambda a_0^3(2 - a_0) + \Lambda a_0^4\left(\Lambda a_0^3 - 3\right) + 3M\right. \\ &\qquad\quad \left.\times (3a_0 - 7M) - 1\right\} w \\ &\qquad \times \left((2\pi a_0)^{-(1+\gamma)} 3a_0^3\right. \\ &\qquad\quad \left.\left.\times \left(3a_0 - 6M - \Lambda a_0^4\right)^{(1+\gamma)/2} - E\right)^{-1-w}\right].\end{aligned} \tag{29}$$

We evaluate the numerical value of a_0 from (28) for $\gamma = 0.2, 0.6, 1$ and check the behavior of solutions by inserting a_0 in (29). We analyze the wormhole stability for static Schwarzschild-de Sitter and anti-de Sitter solutions. The wormhole throat radius a_0 must have the range $r_h < a_0 < r_c$ for the existence of Schwarzschild-de Sitter solution. Static stable and unstable solutions exist if $a_0 > r_h$, $V''(a_0) > 0$ and $V''(a_0) < 0$, respectively. For $a_0 \leq r_h$, there is no static solution which leads to the nonphysical region (grey zone).

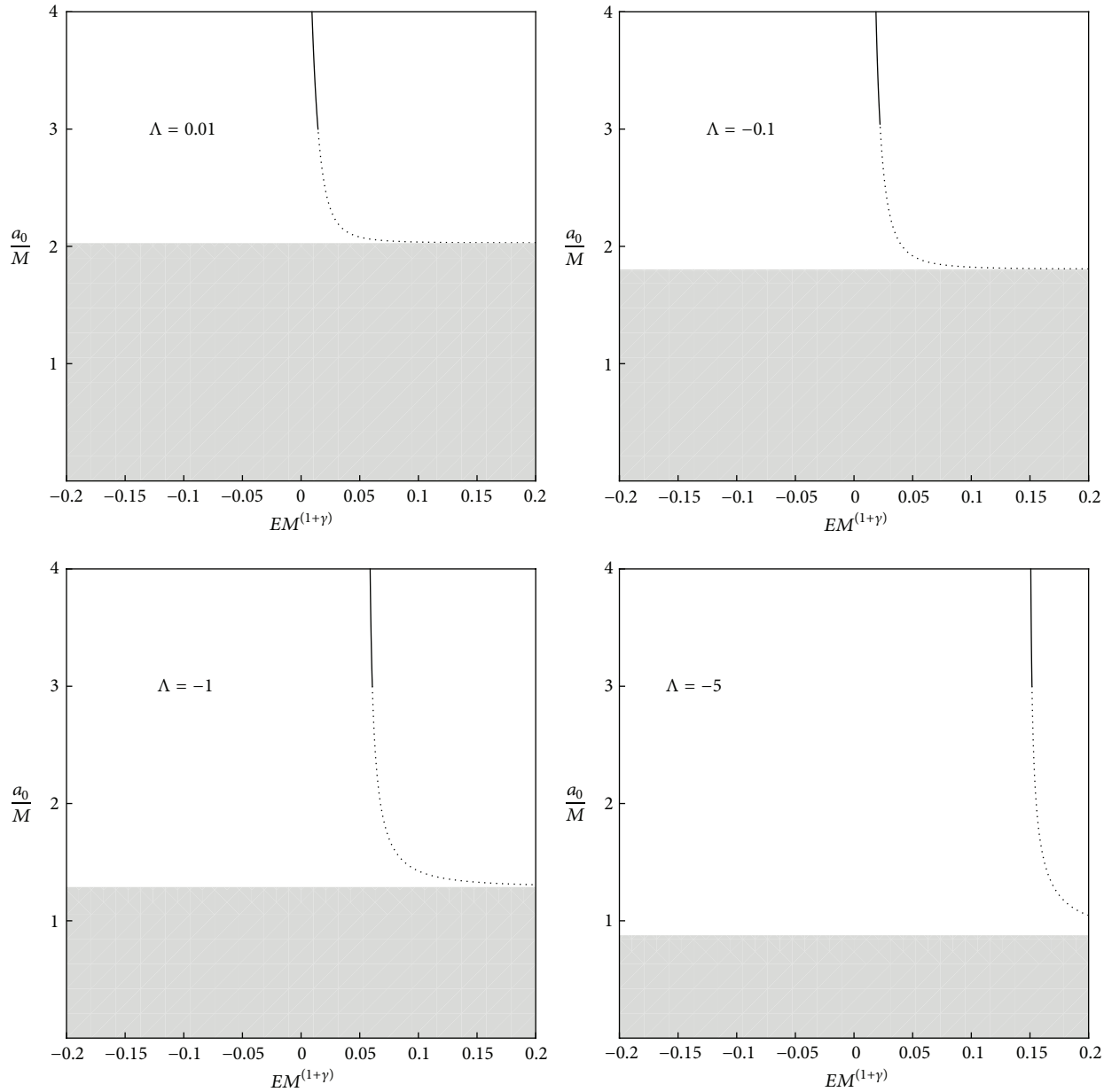

Figure 4: Plots for stable and unstable spherical TSWs with GCCG and the parameters $\gamma = 0.2$, $M = 1$, and $w = -10$.

The unstable and stable wormhole solutions correspond to dotted and solid curves, respectively. The results in Figures 4–6 can be summarized as follows.

(i) Figure 4 for $\Lambda M^2 = 0.01, -0.1, -1, -5$ indicates unstable and stable solutions for both Schwarzschild-de Sitter and anti-de-Sitter TSWs corresponding to $\gamma = 0.2$. These solutions tend to decrease and meet the horizon radius with increasing value of $EM^{(1+\gamma)}$. The horizon radius continues to step down by decreasing the value of Λ.

(ii) For $\gamma = 0.6, 1$, we have two types of solutions (stable and unstable) for $\Lambda M^2 = 0.01, -0.1$, while there exist different solutions for $\Lambda M^2 = -1, -5$; two of them are stable and one is unstable with $\gamma = 1$ as shown in Figures 5 and 6. Here also, the horizon radius continues to decrease as in the previous cases.

4.2. Modified Cosmic Chaplygin Gas. Now we consider MCCG as exotic matter at the wormhole throat. The EoS for MCCG is given by

$$p = A\sigma - \frac{1}{\sigma^{\gamma}}\left[E + \left(\sigma^{1+\gamma} - E\right)^{-w}\right]. \tag{30}$$

Sadeghi and Farahani [28] used MCCG as varying MCCG by assuming E as a function of scale factor a. Here, we assume E as a constant as in the above model. Inserting (15) in (30), we

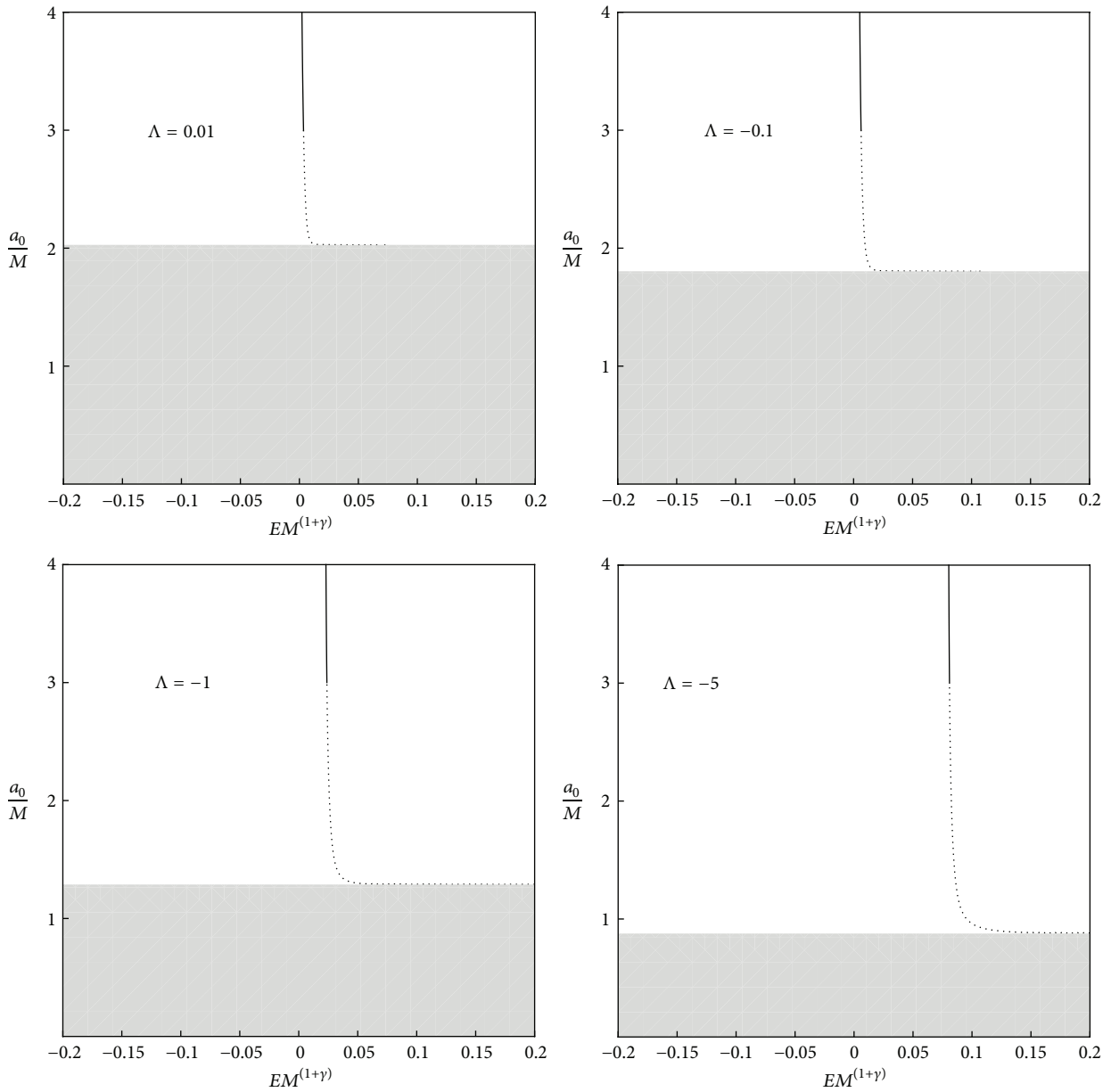

Figure 5: Plots for GCCG with $\gamma = 0.6$, $M = 1$, and $w = -10$.

formulate the corresponding dynamical equation (for static configuration) as

$$\left[a_0^2 G'(a_0) + 2a_0 G(a_0)\right](1+2A)\left[2a_0\right]^{\gamma} - 2\left(4\pi a_0^2\right)^{1+\gamma}\left[G(a_0)\right]^{(1-\gamma)/2} \times \left[E + \left\{(2\pi a_0)^{-(1+\gamma)}\left(G(a_0)\right)^{(1+\gamma)/2} - E\right\}^{-w}\right] = 0. \tag{31}$$

Differentiating (30), we have

$$\sigma'(a) + 2p'(a) = \sigma'(a) \times \left[1 + 2(1+\gamma)\left\{A + w\left(\sigma^{1+\gamma} - E\right)^{-(1+w)}\right\} - \frac{2\gamma p(a)}{\sigma(a)}\right]. \tag{32}$$

The second derivative of $V(a)$ by using (20) and (32) becomes

$$V''(a) = G''(a) - 8\pi^2 \times \left\{\left[\sigma(a) + 2p(a)\right]^2 + 2\sigma(a)\left[\sigma(a) + p(a)\right] \times \left[1 - \frac{2\gamma p}{\sigma} + 2(1+\gamma) \times \left[A + w\left(\sigma(a)^{1+\gamma} - E\right)^{-1-w}\right]\right]\right\}. \tag{33}$$

Inserting the values of $\sigma(a_0)$ and $p(a_0)$, we find that $V(a) = V'(a) = 0$ at $a = a_0$, while (33) turns out to be

$$V''(a_0) = G''(a_0) + \frac{(\gamma-1)\left[G'(a_0)\right]^2}{2G(a_0)} + \frac{G'(a_0)}{a_0}$$

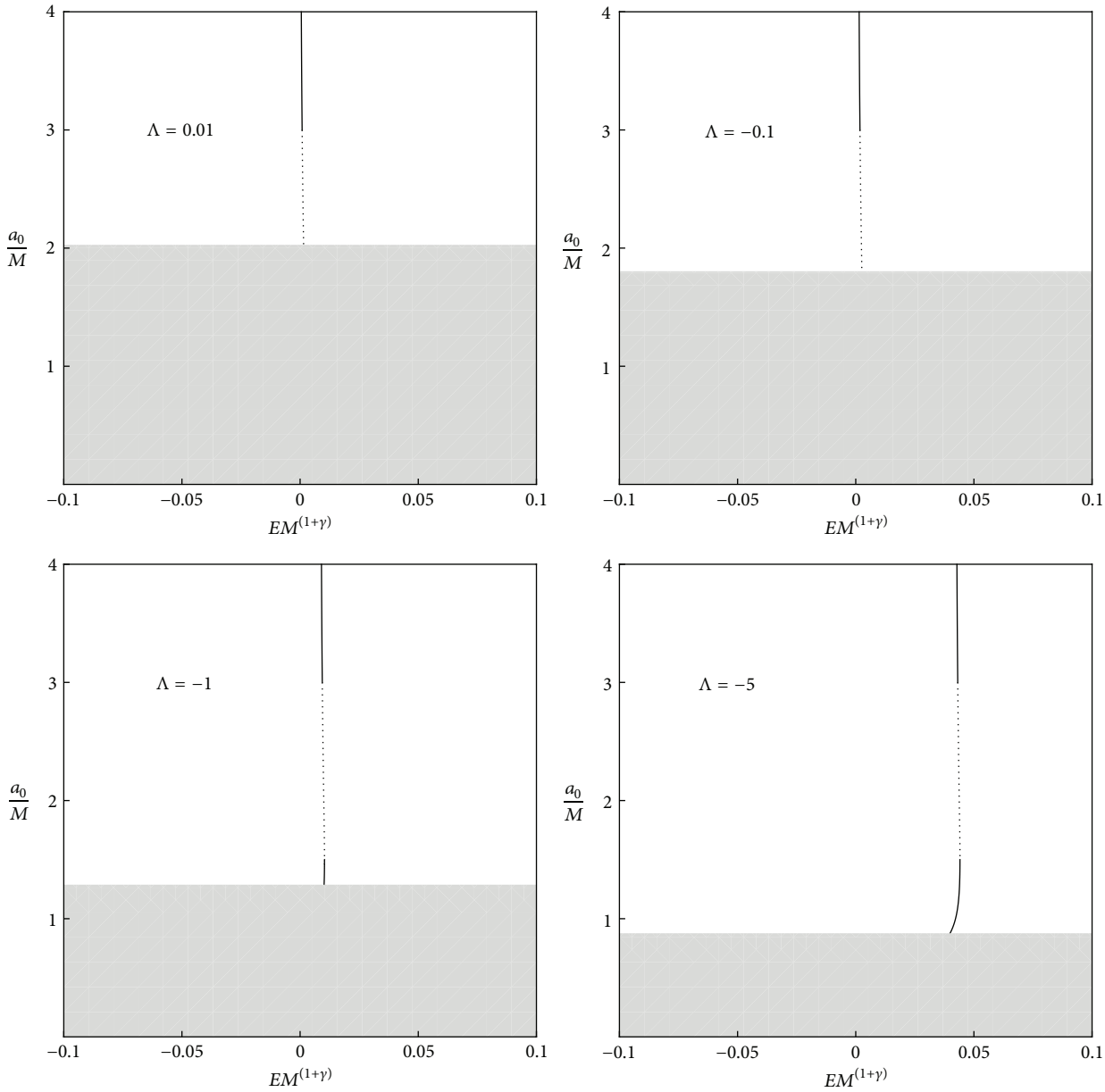

Figure 6: Plots corresponding to GCCG with $\gamma = 1$, $M = 1$, and $w = -10$.

$$\times\left[1+2\left\{A+w(1+\gamma)\left\{\left(\frac{\sqrt{G(a_0)}}{2\pi a_0}\right)^{1+\gamma}-E\right\}^{-(1+w)}\right\}\right]$$

$$-\frac{2G(a_0)}{a_0^2}(1+\gamma)$$

$$\times\left[1+2(1+\gamma)\left[A+w\left\{\left(\frac{\sqrt{G(a_0)}}{2\pi a_0}\right)^{1+\gamma}-E\right\}^{-(1+w)}\right]\right]. \tag{34}$$

For the Schwarzschild-de Sitter and anti-de Sitter wormhole static solutions, (31) takes the form

$$3a_0(1+2A)-3M(1+4A)-2\Lambda a_0^3(1+A)$$

$$-2\left(2\pi a_0\sqrt{3a_0}\right)^{1+\gamma}\left[3a_0-6M-\Lambda a_0^3\right]^{(1-\gamma)/2}$$

$$\times\left[E+\left\{\left(2\pi a_0\sqrt{3a_0}\right)^{-(1+\gamma)}\right.\right.$$

$$\left.\left.\times\left(3a_0^4-6M-\Lambda a_0^3\right)^{(1+\gamma)/2}-E\right\}^{-w}\right]=0. \tag{35}$$

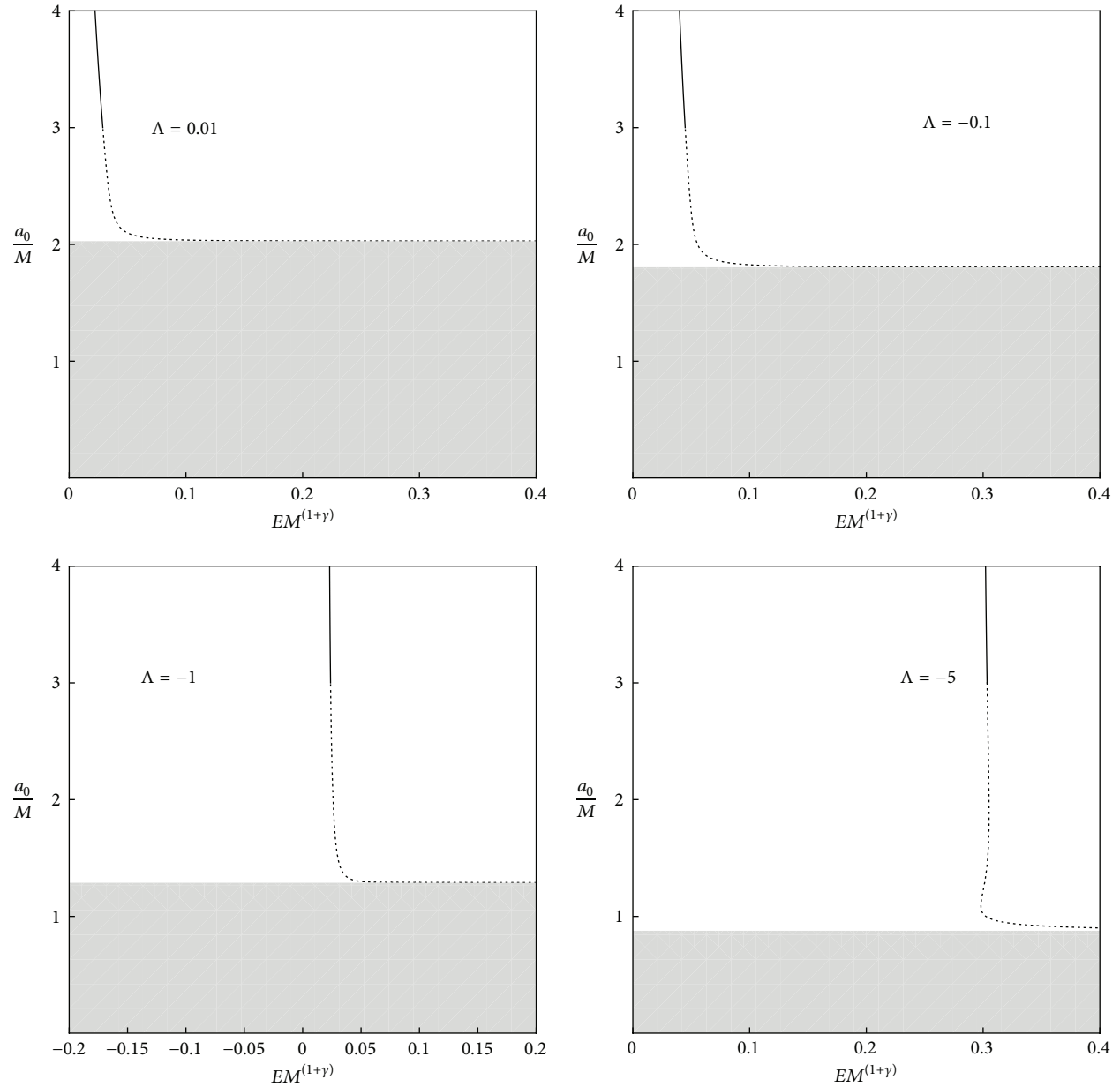

Figure 7: Plots for MCCG with $\gamma = 0.2$, $M = 1$, $A = 2$, and $w = -10$.

By substituting $G(a)$ and $G'(a)$ in (34), $V''(a_0)$ (satisfied by the throat radius) turns out to be

$$\begin{aligned} V''(a_0) &= \frac{2}{3a_0^3\left(3a_0 - 6M - \Lambda a_0^4\right)} \\ &\times \left[9M\Lambda a_0^3\left(2 - a_0\right) + \Lambda a_0^4\left(a_0 - 1\right)\right. \\ &\times \left[6 - \Lambda a_0^2\left(a_0 - 1\right)\right] + 2M\left(a_0 - M\right) - 9a_0^2 + \gamma \\ &\times \left[\Lambda^2 a_0^6\left(1 - a_0^2\right) - 6M\Lambda a_0^3\left(1 + 2a_0\right)\right. \\ &\left. +9M\left(4a_0 - 3M\right) - 9a_0^2\right] \\ &+ 2\left(1 + \gamma\right)\left\{3M\Lambda a_0^3\left(2 - a_0\right) + \Lambda a_0^4\left(\Lambda a_0^3 - 3\right)\right. \\ &\left.\left. +3M\left(3a_0 - 7M\right) - 1\right\} \\ &\times \left[A + w\left(\left(2\pi a_0\right)^{-(1+\gamma)} 3a_0^3\right.\right.\right. \\ &\left.\left.\left. \times \left(3a_0 - 6M - \Lambda a_0^4\right)^{(1+\gamma)/2} - E\right)^{-1-w}\right]\right]. \end{aligned} \tag{36}$$

To discuss the behavior of spherical TSWs with MCCG, we evaluate the numerical value of a_0 from (35) for $\gamma = 0.2, 0.6, 1$ and then substitute it in (36). The results in Figures 7–10 corresponding to $\gamma = 0.2, 0.6, 1$ show stable and unstable

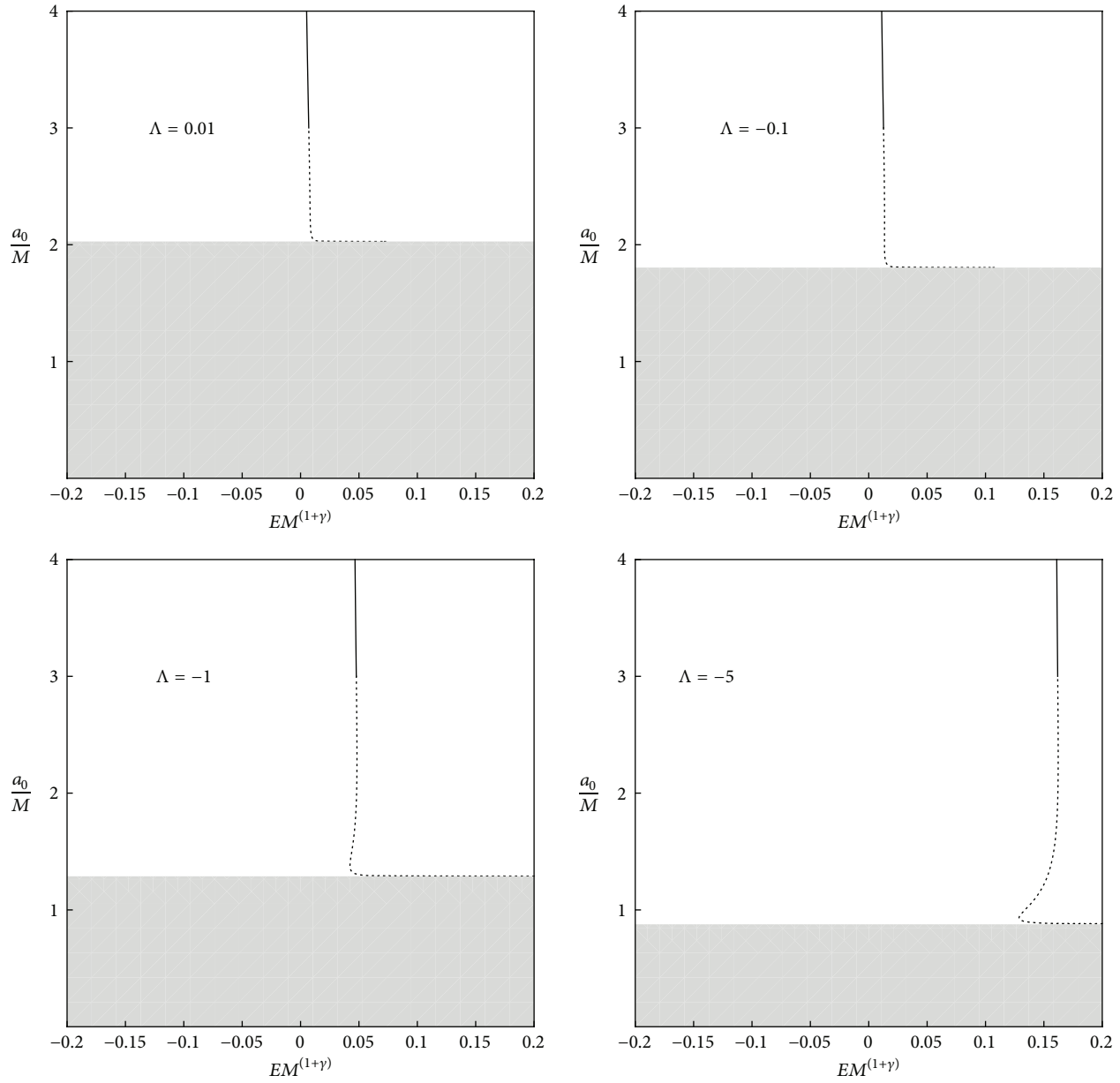

FIGURE 8: Plots corresponding to MCCG with $\gamma = 0.6$, $M = 1$, $A = 2$, and $w = -10$.

wormhole solutions for $\Lambda M^2 = 0.01, -0.1, -1, -5$. In Figures 7 and 8, we find both stable and unstable configurations corresponding to $\gamma = 0.2, 0.6$. These solutions tend to decrease and meet the horizon radius with increasing value of $EM^{(1+\gamma)}$. Similarly, we examine both types of solutions for $\gamma = 1$ (Figures 9-10). The throat radius appears as an increasing function of $EM^{(1+\gamma)}$ for $\Lambda = -5$ and $\gamma = 1$. Moreover, the radius of horizon for the given manifold decreases with small values of ΛM^2.

5. Conclusions

This paper is devoted to construct spherical TSWs with nonvanishing cosmological constant by employing Visser's cut and paste scheme. We have found that the stress-energy tensor components violate the NEC and WEC showing the existence of exotic matter at the throat. We have also examined the attractive and repulsive characteristics of TSWs. A wormhole has attractive nature if $a^r > 0$ which exhibits that an observer should move with an outgoing radial acceleration a^r to avoid being dragged by the wormhole, while it is repulsive for $a^r < 0$; that is, an observer must have the radial acceleration directed towards the inside to keep away from being pushed by the wormhole.

The standard stability approach has been applied by considering two different models of Chaplygin gas as dark energy candidates at the wormhole throat. We have formulated the solutions numerically by solving the dynamical equations

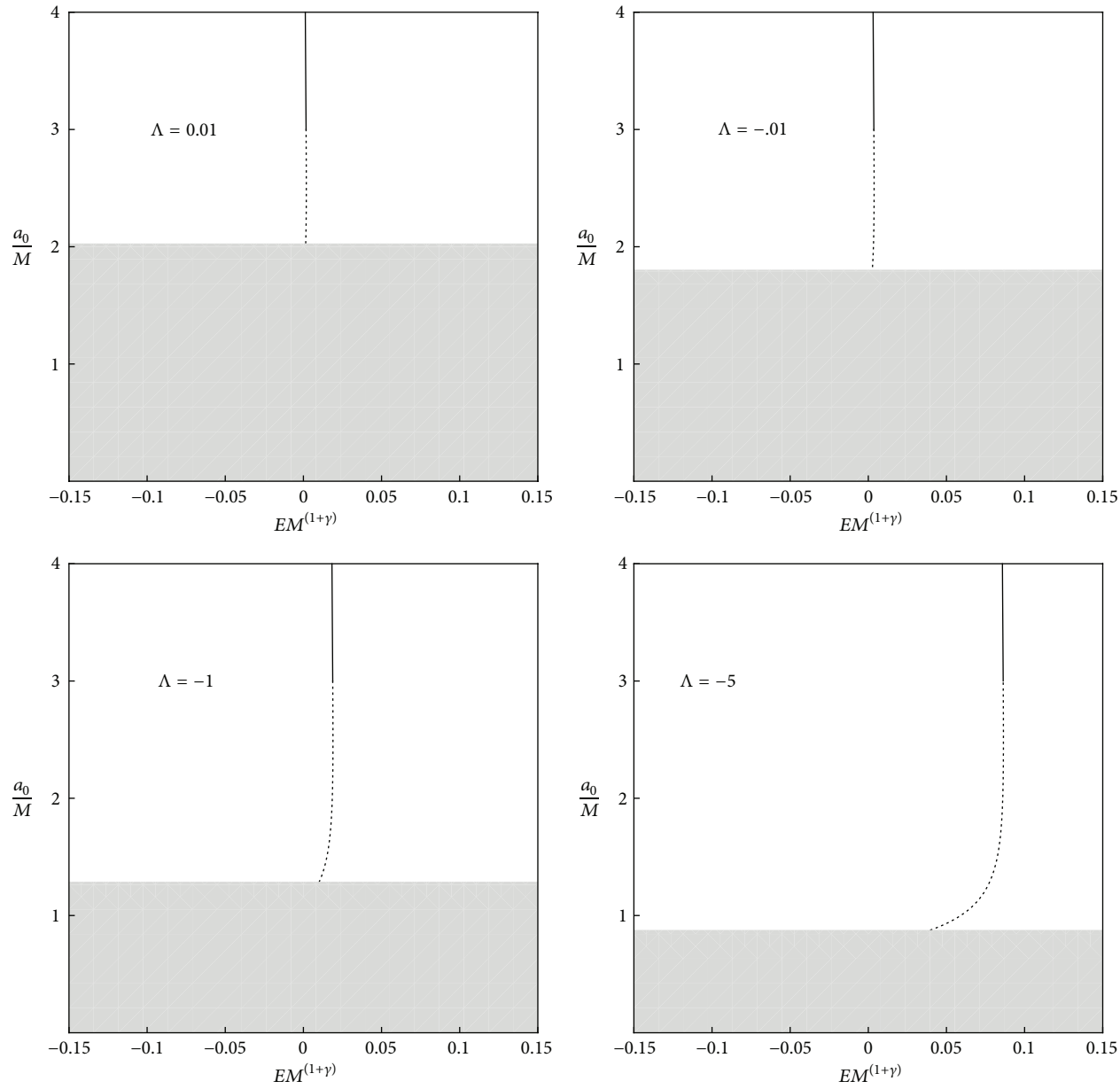

Figure 9: Plots with MCCG corresponding to $\gamma = 1$, $M = 1$, $A = 2$, and $w = -10$.

for $\gamma = 0.2, 0.6, 1$. The results corresponding to GCCG and MCCG for the stability of Schwarzschild-de Sitter and anti-de Sitter configurations are summarized as follows.

(i) Firstly, we have investigated solutions for GCCG corresponding to $\gamma = 0.2, 0.6, 1$. We have found one stable and one unstable static wormhole solution for the given values of γ and $\Lambda M^2 = 0.01, -0.1$. For $\Lambda M^2 = -1, -5$, there exist three types of static solutions (one unstable and two stable) with $\gamma = 1$. For $\gamma = 0.2, 0.6$, the wormhole throat is a decreasing function of $EM^{(1+\gamma)}$ and touches the horizon radius which decreases gradually.

(ii) Secondly, for MCCG, we have both stable and unstable solutions corresponding to both spherical TSW geometries for all values of γ.

Table 1 shows the comparison of solutions for GCCG and MCCG with GCG and MGCG for different values of $\gamma = 0.2, 0.6, 1$. This indicates that the stability of static solutions depends upon the choice of EoS. Here "1S" and "1US" stand for one stable and one unstable solution, respectively. There exist unstable spherical TSW solutions for $\gamma = 0.2, 0.6$ corresponding to GCG [21]. We find that some stable solutions also exist for GCCG and MCCG with $\gamma = 0.2, 0.6$ as compared to GCG. It is worthwhile to mention here that our results for both EoS reduce to [21, 25] in the limit $w \to 0$.

Table 1: Comparison of solutions for different EoS.

Value of γ	EoS	$\Lambda = 0.01$	$\Lambda = -0.1$	$\Lambda = -1$	$\Lambda = -5$
$\gamma = 0.2$	GCG	1US	1US	1US	1US
$\gamma = 0.2$	MGCG	1US	1US	2US	1S
$\gamma = 0.2$	GCCG	1S, 1US	1S, 1US	1S, 1US	1S, 1US
$\gamma = 0.2$	MCCG	1S, 1US	1S, 1US	1S, 1US	1S, 1US
$\gamma = 0.6$	GCG	1US	1US	1US	1S, 2US
$\gamma = 0.6$	MGCG	1US	1US	1S, 2US	1S, 2US
$\gamma = 0.6$	GCCG	1S, 1US	1S, 1US	1S, 1US	1S, 1US
$\gamma = 0.6$	MCCG	1S, 1US	1S, 1US	1S, 1US	1S, 1US
$\gamma = 1$	GCG	1US	1US	1S, 1US	1S, 1US
$\gamma = 1$	MGCG	1S, 1US	1S, 1US	1S, 2US	1S, 1US
$\gamma = 1$	GCCG	1S, 1US	1S, 1US	2S, 1US	2S, 1US
$\gamma = 1$	MCCG	1S, 1US	1S, 1US	1S, 1US	1S, 1US

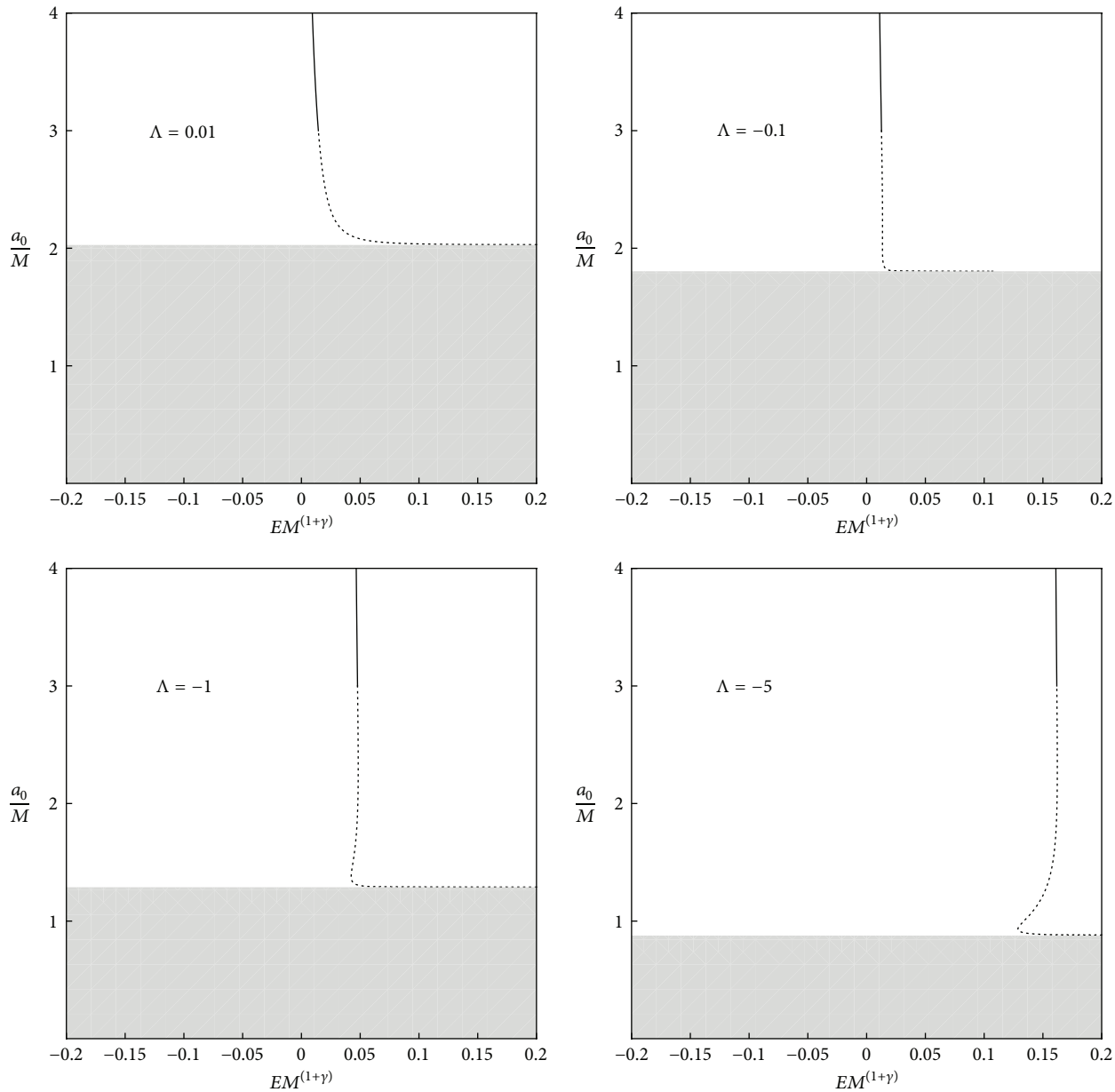

Figure 10: Plots with MCCG corresponding to $\gamma = 1$, $M = 1$, $A = 1$, and $w = 0$.

Conflict of Interests

The authors declare that there is no conflict of interests regarding the publication of this paper.

References

[1] A. Einstein and N. Rosen, "The particle problem in the general theory of relativity," *Physical Review D*, vol. 48, no. 1, pp. 73–77, 1935.

[2] M. S. Morris and K. S. Thorne, "Wormholes in spacetime and their use for interstellar travel: a tool for teaching general relativity," *American Journal of Physics*, vol. 56, no. 5, pp. 395–412, 1988.

[3] G. Darmois, *Memorial des Sciences Mathematics*, Gautheir-Villars, New York, NY, USA, 1927.

[4] W. Israel, "Singular hypersurfaces and thin shells in general relativity," *Il Nuovo Cimento B: 10*, vol. 44, no. 1, pp. 1–14, 1966.

[5] M. Visser, S. Kar, and N. Dadhich, "Traversable wormholes with arbitrarily small energy condition violations," *Physical Review Letters*, vol. 90, no. 20, 2003.

[6] M. Sharif and Z. Yousaf, "Dynamical instability of the charged expansion-free spherical collapse in $f(R)$ gravity," *Physical Review D*, vol. 88, Article ID 024020, 2013.

[7] M. Sharif and M. Z. Bhatti, "Stability of the expansion-free charged cylinder," *Journal of Cosmology and Astroparticle Physics*, vol. 10, article 056, 2013.

[8] E. Poisson and M. Visser, "Thin-shell wormholes: linearization stability," *Physical Review D*, vol. 52, no. 12, pp. 7318–7321, 1995.

[9] F. S. N. Lobo and P. Crawford, "Linearized stability analysis of thin-shell wormholes with a cosmological constant," *Classical and Quantum Gravity*, vol. 21, no. 2, pp. 391–404, 2004.

[10] M. Thibeault, C. Simeone, and E. F. Eiroa, "Thin-shell wormholes in Einstein-Maxwell theory with a Gauss-Bonnet term," *General Relativity and Gravitation*, vol. 38, no. 11, pp. 1593–1608, 2006.

[11] Z. Amirabi, M. Halilsoy, and S. H. Mazharimousavi, "Effect of the Gauss-Bonnet parameter in the stability of thin-shell wormholes," *Physical Review D*, vol. 88, Article ID 124023, 2013.

[12] M. Sharif and Z. Yousaf, "Cylindrical thin-shell wormholes in *f(R)* gravity," *Astrophysics and Space Science*, vol. 351, no. 1, pp. 351–360, 2014.

[13] E. F. Eiroa and C. Simeone, "Cylindrical thin-shell wormholes," *Physical Review D*, vol. 70, no. 4, Article ID 044008, 6 pages, 2004.

[14] M. G. Richarte, "Cylindrical wormholes with positive cosmological constant," *Physical Review D*, vol. 88, Article ID 027507, 2013.

[15] M. Sharif and S. Mumtaz, "Effects of charge on the stability of thin-shell wormholes," *Astrophysics and Space Science*, vol. 352, no. 2, pp. 729–736, 2014.

[16] S. V. Sushkov, "Wormholes supported by a phantom energy," *Physical Review D*, vol. 71, Article ID 043520, 2005.

[17] F. S. N. Lobo, "Phantom energy traversable wormholes," *Physical Review D*, vol. 71, no. 8, Article ID 084011, 2005.

[18] A. Das and S. Kar, "The Ellis wormhole with 'tachyon matter'," *Classical and Quantum Gravity*, vol. 22, no. 14, pp. 3045–3053, 2005.

[19] F. S. N. Lobo, "Chaplygin traversable wormholes," *Physical Review D*, vol. 73, no. 6, Article ID 064028, 9 pages, 2006.

[20] E. F. Eiroa and C. Simeone, "Stability of chaplygin gas thin-shell wormholes," *Physical Review D*, vol. 76, Article ID 024021, 2007.

[21] E. F. Eiroa, "Thin-shell wormholes with a generalized Chaplygin gas," *Physical Review D*, vol. 80, Article ID 044033, 2009.

[22] P. K. F. Kuhfittig, "The stability of thin-shell wormholes with a phantom-like equation of state," *Acta Physica Polonica B*, vol. 41, no. 9, pp. 2017–2029, 2010.

[23] T. Bandyopadhyay, A. Baveja, and S. Chakraborty, "Stability analysis of thin shell wormholes supported by the modified chaplygin gas," *International Journal of Modern Physics D*, vol. 18, no. 13, pp. 1977–1990, 2009.

[24] A. Banerjee, "Stability of charged thin-shell wormholes in (2+1) dimensions," *International Journal of Theoretical Physics*, vol. 52, no. 8, pp. 2943–2958, 2013.

[25] M. Sharif and M. Azam, "Spherical thin-shell wormholes and modified chaplygin gas," *Journal of Cosmology and Astroparticle Physics*, vol. 2013, no. 5, p. 25, 2013.

[26] M. Sharif and M. Azam, "Reissner-Nordström thin-shell wormholes with generalized cosmic Chaplygin gas," *The European Physical Journal C*, vol. 73, p. 2554, 2013.

[27] P. F. González-Díaz, "Tensorial perturbations in the bulk of inflating brane worlds," *Physical Review D*, vol. 68, no. 8, Article ID 084009, 4 pages, 2003.

[28] J. Sadeghi and H. Farahani, "Interaction between viscous varying modified cosmic chaplygin gas and Tachyonic fluid," *Astrophysics and Space Science*, vol. 347, no. 1, pp. 209–219, 2013.